IJCRT.ORG ISSN : 2320-2882

INTERNATIONAL JOURNAL OF CREATIVE RESEARCH THOUGHTS (IJCRT)

An International Open Access, Peer-reviewed, Refereed Journal

ENHANCEMENT OF MELANOMA SKIN CANCER DIAGNOSIS BY MODIFIED DRAGONFLY-BASED NEURAL NETWORK

[1]D.Divya, [2]T.R. GaneshBabu, [3]K.Ananthajothi

[1]Associate Professor, [2]Professor, [3]Associate Professor

[1] Computer Science and Engineering,

[1] Jerusalem College of Engineering, Chennai, India

[2] Electronics and Communication Engineering,

[2]Muthayammal Engineering College, Rasipuram, India

[3]Computer Science and Engineering,

[3]Rajalakshmi Engineering College, Chennai, India

Abstract: Skin cancer, especially melanoma, is a progressing public health burden. Treatment and survival rates improve dramatically when malignant melanoma skin cancer is detected at an early stage. In this study, we use many forms of artificial intelligence to complete the process of diagnosing melanoma. Picture scaling, hair removal, and contrast enhancement are all performed at the pre-processing phase of the input dermoscopic imaging. Next, Fuzzy C-Mean Clustering is used to extract lesions from the image once the data has been pre-processed. Extraction of characteristics from a picture involves eliminating color morphological and morphological transformation features. Furthermore, a Classification model called a Neural Network is used to classify features (NN). In this case, the NN model trained is modified using the Dragonfly Algorithm (MDA). Finally, the analysis is carried on standard datasets and proves the performance of the developed model from diverse performance metrics.

Index Terms **- Melanoma Skin Cancer, Skin Cancer diagnosis, Fuzzy C-Mean Clustering, Neural Network, Modified Dragonfly Algorithm, Color morphological features and morphological transformation features.**

NOMENCLATURE

Abbreviations	Descriptions
FCM	Fuzzy C-Mean Clustering
NN	Neural Network
MDA	Modified Dragonfly Algorithm
BCC	Basal Cell Carcinoma
SCC	Squamous Cell Carcinoma
AUC	Area Under Curve
FDR	False Discovery Rate
PSO	Particle Swarm Optimization
FNR	False Negative Rate
AHE	Adaptive Histogram Equalization
FPR	False Positive Rate
GA	Genetic Algorithm
SVM	Support Vector Machine
NPV	Negative Predictive Value
MCC	Matthew's Correlation Coefficient

I. INTRODUCTION

Cancer is now widely acknowledged as a major killer in the modern world. The early researches have shown that many kinds of skin cancer are existing. Primitive studies confirmed the existence of three primary types of skin cancer: basal cell carcinoma, squamous cell carcinoma, and melanoma. Nevertheless, melanoma is assumed as one of the dangerous signs causing death and its occurrence might gradually improve with respect to time. In fact, Melanoma is a disease that impairs melanin production by slowing the proliferation of melanocyte cells. [6]. Moreover, the skin which has inadequate melanin is vulnerable to the danger of sun burns and hazardous ultra-violet rays from the sun [7]. Many kinds of research specify that the disease needs early intrusion for recognizing the accurate signs, which will make simple for the physicians and dermatologist for averting it [9]. This disorder is proved to be irregular and it is classified by the lesion growth existing in the skin that differs in size, colour, texture and shape [8].

Moreover, Melanoma has a high propensity for developing and even after eliminating the lesions might grow sometimes. It might interrupt and damage the tissues and organs which are very close and attack other regions of the body, which is quite hard to treat. While there is good news for those diagnosed with skin cancer: improved cure rates, the life expectancies for melanoma are lower than those for non-melanoma skin cancer [10]. Doctors usually keep an eye out for skin cancer by visually inspecting their patients often. Moles and other spots that stand out in color from the rest of the skin are what doctors look for during a screening. The process of pictorial monitoring for skin cancer detection won't ensure 100% detection rate and from time to time, it might direct to the impending damage.

In response, a number of approaches were developed for the segmentation and classification of malignancies from dermoscopic imaging. This was done in order to address the concerns. The techniques that have been employed for lesion segmentation is broadly categorized into edge-based, threshold-based and region-based segmentation procedures [11] [12]. There are many research solutions from the development of the computer image analysis models for fast diagnosis of skin cancer in an early stage and solving some of the above mentioned risks [13][33]. Many of the above mentioned approaches were parametric, which means they need information to be distributed normally. These techniques were insufficient for the accurate diagnosis of disease because the nature of the data might not be handled. Retrieving such fine-grained information from benign and malignant skin conditions remains a challenging problem. [14] [15].

The following section will outline the primary contributions that this research work has made.

- To incorporate the combination of intelligent methods for melanoma skin cancer detection using hair removal, contrast enhancement, segmentation of lesion by FCM and classification by NN. Specifically, the training algorithm of NN is enriched by improved meta-heuristic algorithm.
- To mitigate the premature convergence of conventional optimization algorithms by introducing MDA, which could highly, enable the NN classifier to be adaptable for classifying the dermoscopic image into normal or affected.

II. RELATED WORKS

In 2017, Kharazmi *et al.* [1] presented a innovative method for diagnosis and segregating subcutaneous vascular from dermoscopy images pictures. Following this, the vascular features that were recovered from the images were examined in order to categorise the various types of skin cancer. K-Means clustering was utilised so that the haemoglobin constituent could be organised into "standard, pigmented, and erythema zones." As an output of global thresholding, a vessel mask was produced. The efficiency of the suggested technique is validated on the basis of segmentation results, the extraction and determination of vascular features were defined in BCC. The findings demonstrated that the strategy that was proposed achieved the highest AUC in terms of discriminating BCC.

In 2015, Abuzaghleh *et al.* [2] have developed two significant components related to non-invasive real-time automated skin lesion evaluation model to diagnose and prevent melanoma at the starting stage. "Hair identification and elimination, data acquisition, segment, and classification of features were the components that made up the model that was constructed. This proposed model has been evaluated on information culled from Pedro Hispano hospital dermoscopy images using the PH2 database. The test results have shown that the technique was effective in attaining the categorization of atypical, melanoma and benign images.

In 2020, Kadampur and Riyaee [3] have introduced deep learning techniques [31] for categorizing the dermoscopic images for detecting skin cancer. In cloud, a data-driven approach made use of deep learning models for its core applications, which was utilized for building methods that will be useful for predicting the skin cancer by acquiring high accuracy. The developed deep learning approaches were experimented on benchmark datasets and observed the metric AUC of 99.77%.

In 2018, Tan *et al.* [4] have offered a novel prototypical named PSO for skin cancer detection on the basis of dermoscopic images. The recognition of major discriminative features of benign and malignant skin lesions played a significant part in vigorous skin cancer detection. For feature optimization, the suggested PSO technique was used. In order to vary the search procedure, probability distribution and dynamic matrix depictions were employed. By using UCI repository data, different uni-modal and multi-modal standard functions were considered for evaluating the suggested method. These results suggest that the developed model is a highly effective instrument for rapidly identifying skin cancer.

In order to begin identifying the skin lesions, Jaisakthi *et al.* [5] published an automated skin lesion segmentation technique in 2018. Moreover, the suggested technique consisted of two significant phases such as "pre-processing and segmentation". During first phase, the noise like illumination, rulers and hair was eliminated by filtering methods and the skin lesions were segmented in segmentation stage by the GrabCut segmentation algorithm. The proposed technique was assessed on ISIC 2017 challenge database and PH^2 database for validating the performance.

III. PROBLEM STATEMENT

Although there are many methods for detecting and classifying skin cancer diseases, there are still a few inconsistencies with the models that have been built, which means that an effective new strategy for detecting skin cancer needs to be developed. Among them, Random Forest [1] has high performance, and it consumes less time but earns a high computational cost. SVM [2][28] has attained high accuracy, and it is used to find the classifier with minimized error but yet, it is not appropriate for large datasets. Deep learning [3] [27] has high detection accuracy, and it is simple to drag and drop appropriate components for constructing a new model. Still, it requires a large amount of data. PSO [4] offers various alternate velocity update algorithms to permit the extensive exploring of search area and has the capacity to prevent premature convergence of the real PSO procedure. On the other hand, it is quite simple to get stuck in a high-dimensional space's local optimal solution. In addition, the pixels of the captured foreground image are clustered using K-means clustering [5][29], which has resulted in a large Jacquard index and dicing factor. But, in order to improve the accuracy, deep learning models need to be employed. Therefore, the above specified defects might help the researches to develop an effective model for detecting skin cancer.

IV. PROPOSED ARCHITECTURE OF MELANOMA SKIN CANCER

Melanoma, a form of skin cancer that can be very serious and even end in death, is caused by the cumulative effects of a number of distinct factors that have contributed in various ways. The integrated approaches were presented by the conceptual scheme, and Figure 1 provides a graphical depiction of the produced block diagram for the melanoma skin cancer identification process.

There are four primary processes that need to be taken in order to produce a successful detection strategy. These steps are known as "image pre-processing," "segmentation," "feature extraction and classification," and "classification," respectively. The quality of the image is improved during the pre-processing step in order to facilitate the process of locating the image's focal points.

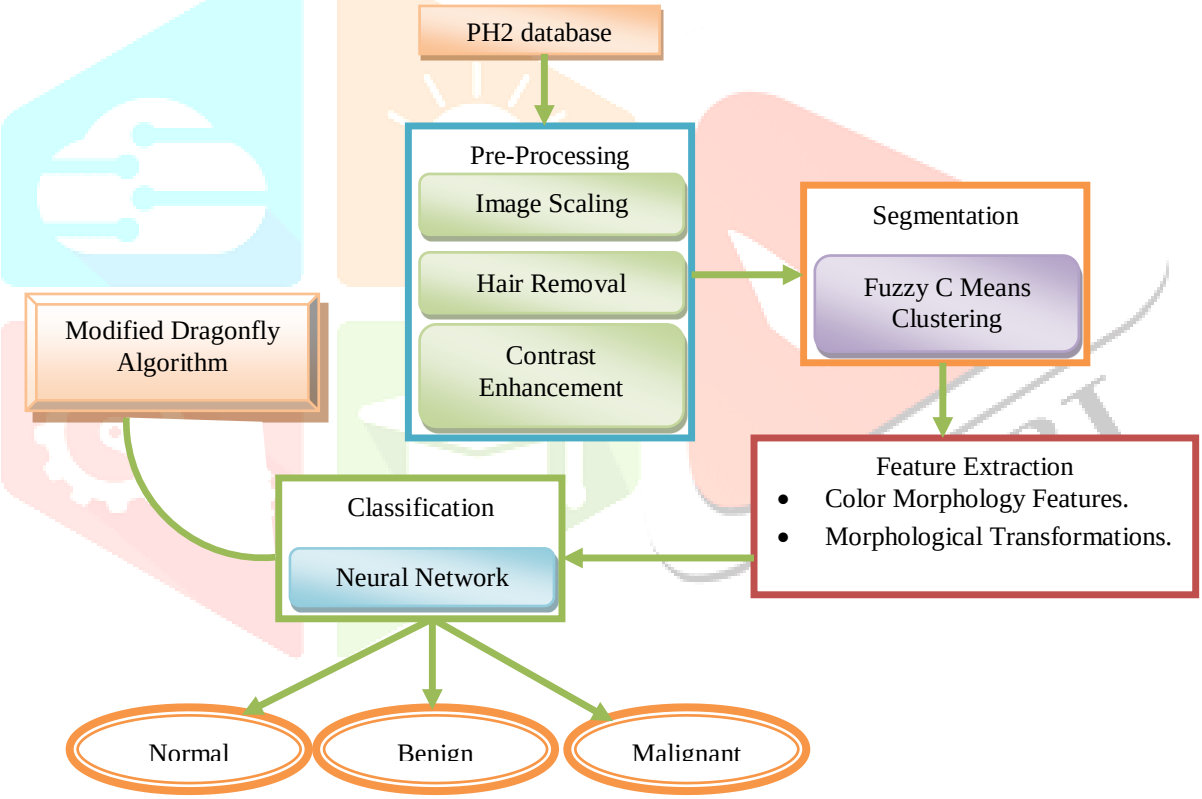

Figure 1 Proposed architecture of skin cancer detection

After that, lesions are extracted from the image by image segmentation using FCM clustering. Two sets of features, based on colour morphogenesis and morphological change, are recovered after the segmentation procedure is complete. The average RGB value, the standard deviation of each RGB value, the lowest and highest RGB values, the size of the wide colour region, and the size of every colour are also obtained, among other colour morphology details. Furthermore, bottom-hat transformations, multi-orientation linear structuring elements, and multi-scale linear structural elements are also taken into account. These characteristics are fed into the detection stage of network neural networks (NN) for accurate skin cancer diagnosis. As an added bonus, MDA can be used to optimize the weight of NN during the classification phase for optimal performance. Optimally trained NN based on MDA seeks to minimize the discrepancy between the observed phenomenon and the predicted result. The goal of this enhancement is to improve diagnostic accuracy so that the image can be properly labelled as "normal," "benign," or "malignant."

4.1 Pre-processing

The fundamental steps carried out in pre-processing are image scaling, hair removal and contrast enhancement. The description of each is given below.

***Scaling*:** It is a representation of the consistent map over all of the pixels of the image and it is represented in Eq. (1). The input image is signified as I_a, and the resizing aspect is represented by $scale$ that will be real or numerical scalar. If the

assortment of $scale$ is exceeding 1, then the resized image I_a^{ims} is bigger than the input image. If the $scale$ is ranging from 0 to 1, then the resized image is lesser than the input image.

$$I_a^{ims} = imresize(I_a, scale) \quad (1)$$

***Hair Removal*:** In order to remove the hair, a morphological operation named image closing is done because it has the capability for eradicating the minute holes existing in the image. The term $I_a^{ims} \bullet HR$ denotes the closing process of the image I_a^{ims} by disk HR , which is signified in Eq. (2).

$$I_a^{mor} = I_a^{ims} \bullet HR = \left(I_a^{ims} \oplus HR\right) \Theta HR \quad (2)$$

After hair removal, the image attained is indicated by I_a^{mor} .

***Contrast Enhancement* [16]:** It is a well-performing approach. Let, A be the computation of gray levels in the input image I_a^{mor} , the real grey level of central pixel c is denoted as a , and the enhanced gray level of central pixel c is denoted as a' . Moreover, the cumulative histogram of central pixel is denoted as B_a . The novel gray level is obtained on the basis of aggregate histogram utility of the actual image according to the condition of AHE. The equation that can be solved mathematically is represented in Eq. (3), where the constant value is represented as w . In addition, the novel gray level value using bitwise shift cumulative histogram for b bits is denoted in Eq. (4).

$$B_a = \sum_{c=0}^{a} Hist(c) = w^2 - \sum_{c=a+1}^{A-1} Hist(c) \quad (3)$$

$$a' = B_a * GL/w^2 = A_a >> b \quad (4)$$

Therefore, the term G_a^{con} denotes the final contrast enhanced image.

V. SEGMENTATION BY FUZZY C MEANS CLUSTERING

The pre-processed image G_a^{con} is used in conjunction with FCM clustering for segmenting the lesion from the image. In the pre-processed image G_a^{con} , the numeral of data points is denoted as ND . Here, the membership function of $i^{th}(1,\cdots,ND)$ vector to $j^{th}(1,\cdots,L)$ is denoted as l_{ij} . The membership values are denoted in Eq. (5). Moreover, Eq. (6) denotes the majorly constrained in order to group the weighed summation of square errors existing in the group. Here, the term $Vec = \{vec_1, vec_2, \cdots, vec_L\}$ refers to the vector of cluster centers and the weighting exponent is specified by m .

$$\forall i, \sum_{j=1}^{L} l_{ij} = 1; \forall i, j, l_{ij} \in [0,1]; \forall j, \sum_{i=1}^{ND} l_{ij} > 0 \quad (5)$$

$$T_m = \sum_{i=1}^{ND} \sum_{j=1}^{L} l_{ij}^m \left\| s_i - vec_j \right\|^2 \quad (6)$$

Moreover, FCM [21] is the local search technique for the clustering mechanism. It is employed as a local search in order to resolve the problem and modeled to differentiate the actual positions of cluster centers. Thus, the FCM clustering gives G^{seg} as the final segmented image.

VI. FEATURE EXTRACTION

In this section, the colour morphology characteristics and morphological modifications are determined.

***Colour Morphology Features*:** These are resolute on the basis of [17][30]. The first three colour features considered are minimum and maximum, standard deviation and average of RGB values. Moreover, the proportion of EUD to the square root of R_{LS} is termed as the color eccentricity and it is given in Eq. (7). Here, the Euclidean distance is denoted as EUD between the centroid of both lesion and biggest color area, and the region of lesion is denoted as R_{LS} .

$$ECC = EUD/\sqrt{R_{LS}} \quad (7)$$

The normalized sum of whole nd regions of specific color CL_d with respect to R_{LS} is referred as relative size RLS of unique color and it is given in Eq. (8).

$$RLS = \sum_{d=1}^{nd} CL_d / R_{LS} \quad (8)$$

Moreover, the normalization of $CL_{\max}$ with respect to R_{LS} is termed as relative size of RLS_{LS} largest color region and it is denoted in Eq. (9).

$$RLS_{LS} = CL_{\max} / R_{LS} \quad (9)$$

Therefore, the features that have been discussed thus far are presumed to be the color morphological features.

***Morphological Transformations*:** Here, six features can be defined by the "top-hat and bottom-hat transformation" based techniques. The bottom-hat transformation is denoted in Eqs. (10) and (11), in which the input gray scale segmented image

is referred as I_{gre}^{sg} and the closing function is indicated by $\bullet$, the linear configuring element $e \in \{3,7,11,15,19,23\}$ is denoted as LS_e, where the measurement of the structuring item is well-defined by e, the bottom-hat transformation is represented as C_e, and the angular rotation is signified as $\theta \in D, D = \{x | 0 \le x \le \pi, x \bmod(\pi/12) = 0\}$.

$$C_e^{\theta} = I_{gre}^{sg} \bullet LS_e^{\theta} - I_{gre}^{sg} \tag{10}$$

$$C_e = \sum_{\theta \in D} C_i^{\theta} \tag{11}$$

Finally, the features extracted are denoted as FR_{com} and it is further subjected to NN.

VII. NEURAL NETWORK

There are three distinct layers in NN [19][32], including the input layer p, the output layer r, and the hidden layer q. Eq. (12) and Eq. (13) represent the results of the hidden layer and the output layer, respectively. Both the input characteristics FR_{com} and the activation function are symbols with acv, and respectively. Both the bias weight of the hidden neurons and the bias weight of the output neurons are denoted by $\tilde{J}_{(\hat{G}q)}^{(E)}$ and $\tilde{J}_{(\hat{G}r)}^{(H)}$, respectively. The input-to-hidden mass transfer and the hidden-to-output mass transfer are denoted by $\tilde{J}_{(pq)}^{(E)}$ and $\tilde{J}_{(qr)}^{(H)}$, correspondingly.

$$\overline{E}^{(E)} = acv\left(\tilde{J}_{(\hat{G}q)}^{(E)} + \sum_{p=1}^{In(CO)} \tilde{J}_{(pq)}^{(E)} FR_{com}\right) \tag{12}$$

$$\hat{H}_r = acv\left(\tilde{J}_{(\hat{G}r)}^{(H)} + \sum_{q=1}^{HN} \tilde{J}_{(qr)}^{(H)} \overline{E}^{(E)}\right) \tag{13}$$

Moreover, the weight function $E_{we}^{NN} = \left\{\tilde{J}_{(\hat{G}q)}^{(E)}, \tilde{J}_{(\hat{G}r)}^{(H)}, \tilde{J}_{(pq)}^{(E)}, \tilde{J}_{(qr)}^{(H)}\right\}$ is selected optimally for providing better training to NN as expressed in Eq. (14).

$$MR = \left\{\tilde{J}_{(\hat{G}q)}^{(E)}, \tilde{J}_{(\hat{G}r)}^{(H)}, \tilde{J}_{(pq)}^{(E)}, \tilde{J}_{(qr)}^{(H)}\right\}^{\arg\min} \sum_{r=1}^{H(CO)} \left|H_r - \hat{H}_r\right| \tag{14}$$

Here, Eq. (14) is the foremost objective function of the proposed prototypical, which is attained by optimizing weight function by MDA. The above equation is the measured error, in which the measured and the actual outcomes are indicated by H_r and $\hat{H}_r$, respectively. By using the proposed MDA, the error difference should be minimized.

7.1 Conventional Dragonfly Algorithm

In the proposed model, the machine learning algorithm NN is improved by MDA, which could be applicable for melanoma skin cancer detection. The behaviours of swarming, either whether static or dynamic, served as the primary source of motivation for DA [20]. The relevance of the swarming is that it is hunting for food, and it should deflect the attention of the adversaries. Cohesiveness, alignments, isolation, attractiveness, and distractions are the five key parameters that are taken into consideration when updating the location of individuals in swarms, and the equations relating to these elements are listed below.

$$Coh_g = \frac{\sum_{h=1}^{M} K_h}{M} - K \tag{15}$$

$$A\ln_g = \frac{\sum_{h=1}^{M} Vel_h}{M} \tag{16}$$

$$Sep_g = -\sum_{h=1}^{M} (K - K_h) \tag{17}$$

$$ATT_g = Food - K \tag{18}$$

$$DST_g = Enemy + K \tag{19}$$

In the above equations, the dragonfly is denoted as g, the term K_h refers the position of h^{th} neighboring distinct and the computation of neighboring individuals is represented as M. The velocity of h^{th} distinct is denoted as Vel_h. Moreover, the source of the food is represented as $Food$ and the location of enemy is signified as $Enemy$.

Moreover, the terms position (K) and step (ΔK) are the two vectors required to be occupied to bring up-to-date the positions of dragonflies. Each dragonfly's action is moving by step vector and it is given in Eq. (20). Here, the weights of cohesion, alignment, separation are indicated by ch, ag, sp correspondingly. The food and enemy factors are denoted as at, and ds individually. The inertia weight is denoted as δ, the current iteration is denoted as it. Eq. (21) specifies the position vector.

$$\Delta K_{it+1} = \left(spSep_g + agA\ln_c + chCoh_g + atATT_g + dsDST_g\right) + \delta \bullet \Delta K_{it} \tag{20}$$

$$K_{it+1} = K_{it} + \Delta K_{it+1} \tag{21}$$

If there isn't a solution in the surrounding area, the dragon fly will have to wander across the search area using random walk, which will increase the randomization and unpredictable qualities while also increasing the amount of investigation. The

following formulae are used to make the necessary adjustments to the dragonfly now, in which the position vector is represented as dpv, random quantities ranges in between 0 and 1 are denoted as rnd_1 and rnd_2 and the term ξ indicates constant.

$$K_{it+1} = K_{it} + Levy(dpv) \times K_{it} \tag{22}$$

$$Levy(dpv) = 0.01 \times \frac{rnd_1 \times \phi}{\left|rnd_2\right|^{\frac{1}{dpv}}} \tag{23}$$

$$\phi = \left(\frac{\Gamma(1+\xi) \times \sin\left(\frac{\Pi\xi}{2}\right)}{\Gamma\left(\frac{1+\xi}{2}\right) \times \xi \times 2^{\left(\frac{\xi-1}{2}\right)}} \right)^{\frac{1}{\xi}} \tag{24}$$

$$\Gamma(k) = (k-1)! \tag{25}$$

Calculating the average Euclidean distance between all of the dragonflies enables one to establish the general area in which each dragonfly resides and later the update of K and ΔK is done.

VIII. PROPOSED MDA

The inspiration of DA is on the basis of static and dynamic behaviour of dragonflies. However, the traditional DA is having few conflicts such as unbalance exploration and exploitation, and premature convergence. In order to improve the performance, trial is considered to check the performance. In the event that the solution does not show any signs of progress during any iteration, trial of 1 is incremented. So, in order to update the solution in different aspect, trial is checked, and if trial is larger than or equal to 5, and then levy update is performed in the proposed MDA despite of conventional DA. Algorithm 1 portrays the stepwise operation of developed MDA.

Algorithm 1: Proposed MDA

The entire solutions of dragonflies K need to be initialized
Initialize step vectors ΔK
while the last necessary condition is not met
  Update source of food & enemy
    update δ, sp, ag, ch, at, and ds
  Compute Sep, Aln, Coh, ATT, and DsT
  Update the distance between residents
  If trial<5
    Eq. (20) serve to revise velocity vectors
    Eq. (21) enables vector position updates
  Else
    Eq. (22) is computed in order to upgrade the solution
  end if
  Feasibility analysis should be used to examine the revised response
end while

IX. RESULTS AND DISCUSSIONS

8.1 Experimental Results

The proposed skin cancer recognition was simulated in MATLAB 2018a and the presentation evaluation was done. The dataset considered for the experiment was taken from the URL "(https://www.fc.up.pt/addi/ph2%20database.html", Access date: 2020-01-07). The performance evaluation of the proposed MDA was associated over existing models like SVM [24], NN [19], GA-NN [23], PSO-NN [22] and DA-NN [20] for the relevant performance measures.

8.2 Segmented Results

Figure 2 shows the pre-processed and segmented results of the developed skin cancer diagnosis model.

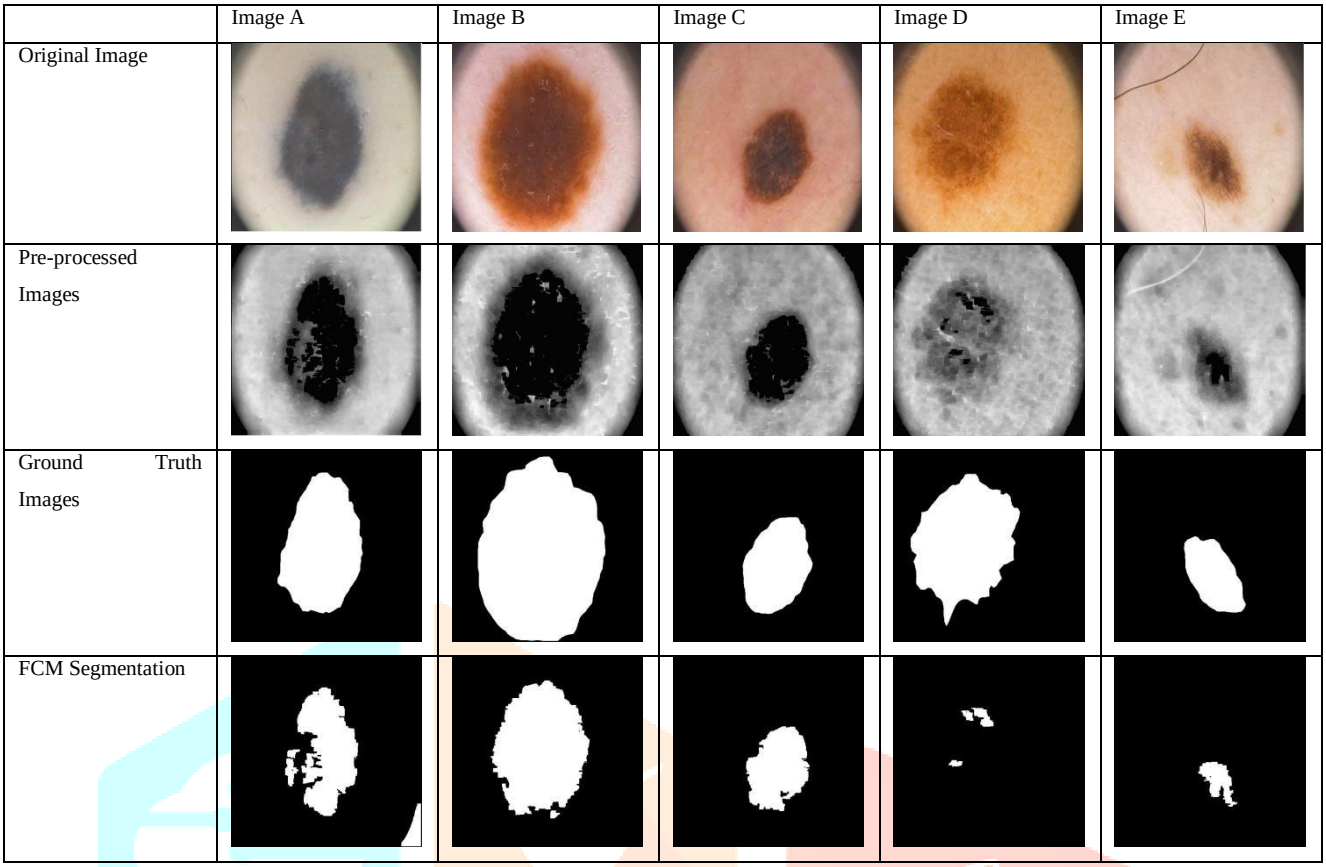

Figure 2 Segmentation of the developed skin cancer diagnosis

8.3 Performance Analysis

Figure 3 illustrates both the effectiveness of the new MDA-NN algorithm as well as the efficacy of the existing techniques. From the bar chart analysis, it is seen that the accurateness of the enhanced MDA-NN is 72.9% improved than DA, 43.1% improved than PSO-NN, 36% improved than GA-NN and NN and 53% improved than SVM. And furthermore, the precision of the MDA-NN that was implemented is 16.8% superior to DA and NN, 15.4% higher than PSO-NN, 7.7% higher than GA-NN and 19.7% higher to SVM. From the results, it is confirmed that the presented MDA-NN is superior in detecting the skin cancer.

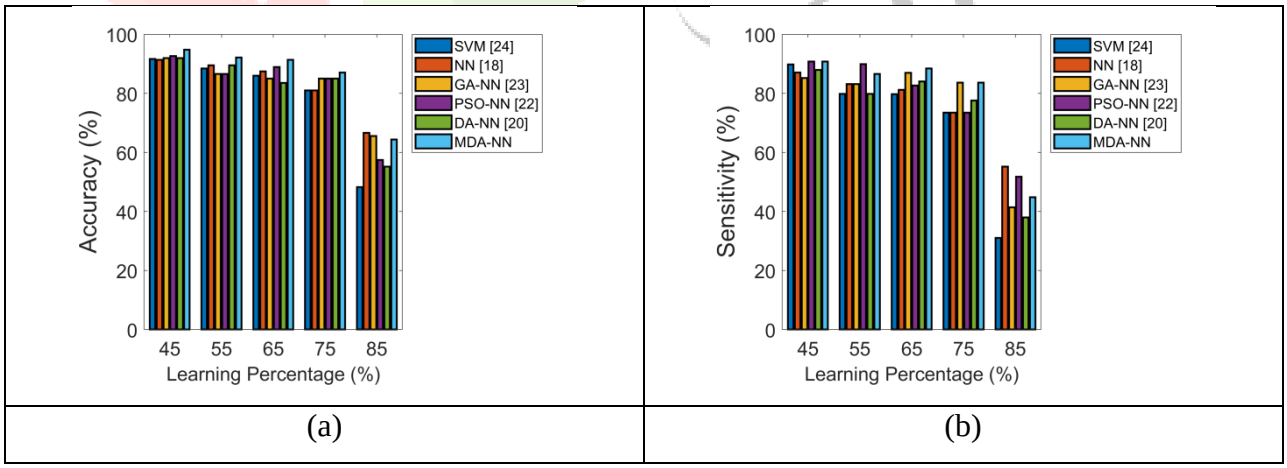

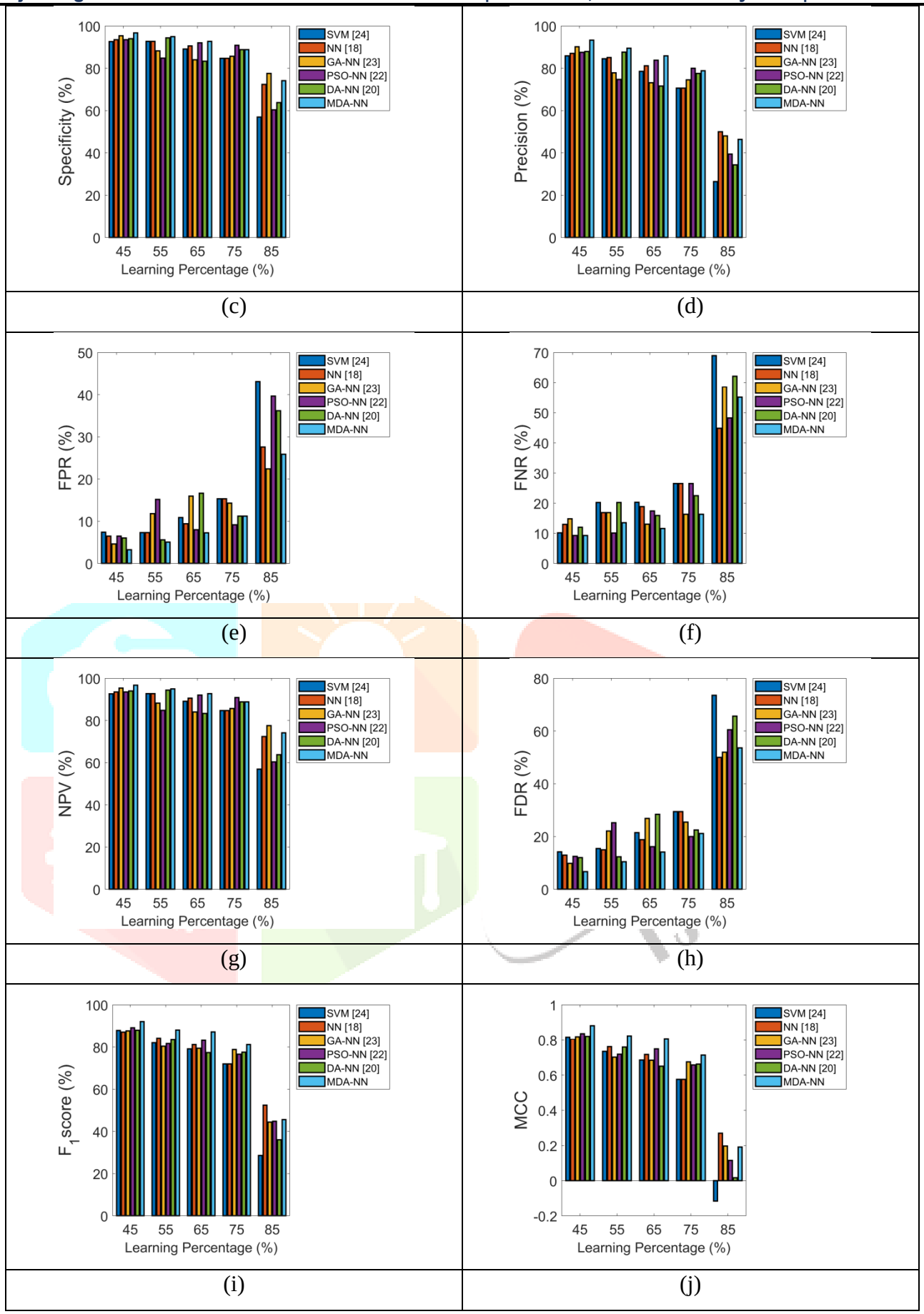

Figure 3 Performance analysis of Parametric measures like (a) accuracy, (b) sensitivity, (c) specificity, (d) precision, (e) FPR, (f) FNR, (g) NPV, (h) FDR, (i) F1 score and (j) MCC

8.3 Comparative Exploration on Different Classifiers

Analyses of the classification performance of the proposed MDA are compared to those of well-known classifiers shown in Table 1. The enhanced MDA-NN outperforms the SVM and NN in terms of accuracy by.5%, while it outperforms GA-NN, PSO-NN, and DA-NN by 2.4%. The created MDA outperforms SVM and NN in terms of accuracy by 11.6%, GA-NN by 5.4%, PSO-NN by 1.4%, and DA-NN by 1.6%. This means the newly improved MDA is effective at spotting cases of skin cancer.

Table 1 Analysis on diverse classifiers

Performance Measures	SVM [24]	NN [18]	GA-NN [23]	PSO-NN [22]	DA-NN [20]	MDA-NN
Accuracy	0.80952	0.80952	0.85034	0.85034	0.85034	0.87075
Specificity	0.84694	0.84694	0.85714	0.90816	0.88776	0.88776
Sensitivity	0.73469	0.73469	0.83673	0.73469	0.77551	0.83673
FPR	0.15306	0.15306	0.14286	0.091837	0.11224	0.11224
NPV	0.84694	0.84694	0.85714	0.90816	0.88776	0.88776
Precision	0.70588	0.70588	0.74545	0.8	0.77551	0.78846
FNR	0.26531	0.26531	0.16327	0.26531	0.22449	0.16327
MCC	0.57602	0.57602	0.67596	0.65754	0.66327	0.7143
F1 score	0.72	0.72	0.78846	0.76596	0.77551	0.81188
FDR	0.29412	0.29412	0.25455	0.2	0.22449	0.21154

X. CONCLUSION

The model for the identification of skin cancer that was developed contained the procedures of "pre-processing," "segmentation," "feature extraction," and "classification." The dermoscopic image that was being read in was subjected to a series of pre-processing operations, some of which included scaling the image, removing hair, and increasing contrast. Following that, the FCM clustering method was applied in order to successfully complete the lesion segmentation. After the process of segmentation was finished, a number of features, such as those pertaining to color morphology and morphological transformation, were extracted. After that, NN was applied to do classification based on the obtained characteristics, and the results were examined. The training model of the NN was able to be improved with the help of the MDA that was proposed. According to the findings, the accuracy of the improved MDA-NN is.5% better than that of the NN and SVM, and it is 2.4% better than that of the GA-NN, PSO-NN, and DA-NN respectively. As a direct consequence of this, one can reach the inference that the MDA-NN that was suggested is appropriate for the diagnosis of skin cancer.

REFERENCES

[1] P. Kharazmi, M. I. AlJasser, H. Lui, Z. J. Wang and T. K. Lee, "Automated Detection and Segmentation of Vascular Structures of Skin Lesions Seen in Dermoscopy, With an Application to Basal Cell Carcinoma Classification," IEEE Journal of Biomedical and Health Informatics, vol. 21, no. 6, pp. 1675-1684, Nov. 2017.

[2] O. Abuzaghleh, B. D. Barkana and M. Faezipour, "Noninvasive Real-Time Automated Skin Lesion Analysis System for Melanoma Early Detection and Prevention," IEEE Journal of Translational Engineering in Health and Medicine, vol. 3, pp. 1-12, 2015.

[3] Mohammad AliKadampur, and SulaimanAl Riyaee, "Skin cancer detection: Applying a deep learning based model driven architecture in the cloud for classifying dermal cell images", Informatics in Medicine Unlocked, vol.18, 2020.

[4] Teck YanTan, LiZhang, Siew ChinNeoh, and Chee PengLim, "Intelligent skin cancer detection using enhanced particle swarm optimization", Knowledge-Based Systems, vol.158, pp.118-135, 15 October 2018.

[5] S. M. Jaisakthi, P. Mirunalini and C. Aravindan, "Automated skin lesion segmentation of dermoscopic images using GrabCut and K-means algorithms," IET Computer Vision, vol. 12, no. 8, pp. 1088-1095, 12, 2018.

[6] S. Suer, S. Kockara, and M. Mete, "An improved border detection in dermoscopy images for density based clustering," BMC Bioinformat., vol. 12, no. 10, 2011.

[7] M. Rademaker and A. Oakley, "Digital monitoring by whole body photography and sequential digital dermoscopy detects thinner melanomas," J. Primary Health Care, vol. 2, no. 4, pp. 268-272, 2010

[8] Q. Abbas, I. F. Garcia, M. E. Celebi, and W. Ahmad, "A feature-preserving hair removal algorithm for dermoscopy images," Skin Res. Technol., vol. 19, no. 1, pp. 27-36, 2013

[9] K. Kiani and A. R. Sharafat, "E-shaver: An improved DullRazor for digitally removing dark and light-colored hairs in dermoscopic images," Comput. Biol. Med., vol. 41, no. 3, pp. 139-145, 2011.

[10] E. Ahn et al., "Saliency-Based Lesion Segmentation via Background Detection in Dermoscopic Images," IEEE Journal of Biomedical and Health Informatics, vol. 21, no. 6, pp. 1685-1693, Nov. 2017.

[11] M. Emre Celebi, Gerald Schaefer, Hitoshi Iyatomi, and William V. Stoecker, "Lesion border detection in dermoscopy images", Comput. Med. Imaging Graph., vol.33, no.2, pp. 148– 153, 2009.

[12] M. Silveira et al., "Comparison of Segmentation Methods for Melanoma Diagnosis in Dermoscopy Images," IEEE Journal of Selected Topics in Signal Processing, vol. 3, no. 1, pp. 35-45, Feb. 2009.

[13] Esteva A, Kuprel B, Novoa RA, Ko J, Swetter SM, Blau HM, and Thrun S, "Dermatologist-level classification of skin cancer with deep neural networks", Nature, vol.542, no. 7639, pp. 115-118, 2017.

[14] F. Xie, H. Fan, Y. Li, Z. Jiang, R. Meng and A. Bovik, "Melanoma Classification on Dermoscopy Images Using a Neural Network Ensemble Model," IEEE Transactions on Medical Imaging, vol. 36, no. 3, pp. 849-858, March 2017.

[15] K. Shimizu, H. Iyatomi, M. E. Celebi, K. Norton and M. Tanaka, "Four-Class Classification of Skin Lesions With Task Decomposition Strategy," IEEE Transactions on Biomedical Engineering, vol. 62, no. 1, pp. 274-283, Jan. 2015.

[16] Z. Wang and J. Tao, "A Fast Implementation of Adaptive Histogram Equalization," 2006 8th International Conference on Signal Processing, Beijing, 2006.

[17] S. W. Menzies et al., "An atlas of surface microscopy of pigmented skin lesions: dermoscopy", McGraw-Hill Roseville, 2003.

[18] F. Fernández-Navarro, M. Carbonero-Ruz, D. Becerra Alonso and M. Torres-Jiménez, "Global Sensitivity Estimates for Neural Network Classifiers," IEEE Transactions on Neural Networks and Learning Systems, vol. 28, no. 11, pp. 2592-2604, Nov. 2017.

[19] M. Marsaline Beno, Valarmathi I. R, Swamy S. M and B. R. Rajakumar, "Threshold prediction for segmenting tumour from brain MRI scans", International Journal of Imaging Systems and Technology, Vol. 24, No. 2, pages 129-137, 2014.

[20] Mohammad Jafari, and Mohammad Hossein Bayati Chaleshtari, " Using dragonfly algorithm for optimization of orthotropic infinite plates with a quasi-triangular cut-out", European Journal of Mechanics A/Solids, vol. 66, pp.1-14, 2017.

[21] Weina Wang, Yunjie Zhang, Yi Li and Xiaona Zhang,"The Global Fuzzy C-Means Clustering Algorithm," 2006 6th World Congress on Intelligent Control and Automation, Dalian, pp. 3604-3607, 2006.

[22] M.E.H.Pedersen, and A.J.Chipperfield, "Simplifying Particle Swarm Optimization", Applied Soft Computing, vol.10, no.2, pp.618-628, March 2010.

[23] SeyedaliMirjalili, Seyed MohammadMirjalili, and AndrewLewis, "Grey Wolf Optimizer", Advances in Engineering Software, vol.69, pp.46-61, March 2014.

[24] A.H.Gandomi, X.-S.Yang, S.Talatahari, and A.H.Alavi, "Firefly algorithm with chaos", Communications in Nonlinear Science and Numerical Simulation, vol.18, no.1, pp.89-98, January 2013.

[25] ShuangYu, Kok KiongTan, Ban LeongSng, Shengjin, and Alex Tiong HengSia, "Lumbar Ultrasound Image Feature Extraction and Classification with Support Vector Machine", Ultrasound in Medicine & Biology, vol.41, no.10, pp.2677-2689, October 2015.

[26] S. M. Swamy, B. R. Rajakumar and I. R. Valarmathi, "Design of Hybrid Wind and Photovoltaic Power System using Opposition-based Genetic Algorithm with Cauchy Mutation", IET Chennai Fourth International Conference on Sustainable Energy and Intelligent Systems (SEISCON 2013), Chennai, India, Dec. 2013.

[27] Ananthajothi, K., Subramaniam, M. Multi level incremental influence measure based classification of medical data for improved classification. Cluster Comput 22, 15073–15080 (2019). https://doi.org/10.1007/s10586-018-2498-z

[28] Subramaniam & M Ananthajothi, K, 'Efficient Classification of Medical data and Disease Prediction using Multi Attribute Disease Probability Measure', Applied Mathematics & Information Sciences, ISSN 1935-0090, E.ISSN 2325-0399, Vol. 13, no. 5, pp. 783-789 (2019).https://doi:10.18576/amis/130511

[29] Ananthajothi, K & Subramaniam, M , 'CLDC: Efficient Classification of Medical Data Using Class Level Disease Convergence Divergence Measure', International Journal of Innovative Technology and Exploring Engineering (IJITEE), ISSN 2278-3075, Vol. 8, no. 10, pp. 2256-2262 (2019).https://doi:10.35940/ijitee.J1123.0881019.

[30] D. Divya & T. R. Ganeshbabu, 'Fitness adaptive deer hunting-based region growing and recurrent neural network for melanoma skin cancer detection', Int J Imaging Syst Technol., pp.1–22, 2020, DOI: 10.1002/ima.22414.

[31] D. Divya & T. R. Ganeshbabu, 'An Empirical Study of Melanoma Detection And Its Deep Learning Classifiers', Journal of Critical Reviews, VOL 7, ISSUE 15, ISSN- 2394-5125, 2020.

[32] K. Karthikayani , T. Selvakumar , K. Ananthajothi. "Design of Convolutional Neural Network for Lung Cancer Diagnosis". Annals of the Romanian Society for Cell Biology, Apr. 2021, pp. 7630 -, https://www.annalsofrscb.ro/index.php/journal/article/view/3417.

[33] Sangeetha SKB & Ananthajothi K 2020, 'Machine Learning Tools for Digital Pathology – The Next Big Wave in Medical Science' Solid State Technology, ISSN 0038-111X, Vol. 64, no. 4, pp. 3732-3749.